VOL. 18, NO. 16, AUGUST 2023 ISSN 1819-6608
ARPN Journal of Engineering and Applied Sciences

www.arpnjournals.com

SYSTEMATIC REVIEW OF VARIOUS 3D VOLUMECONSTRUCTION ALGORITHMS ADOPTED IN ISOCENTRIC C-ARM DEVICES

S. Rajkumar[1], R. Divya[1] and V. Sapthagirivasan[1, 2]
[1]Department of Biomedical Engineering, Rajalakshmi Engineering College, Chennai, India
[2]Department of Medical Devices and Healthcare Technologies, IT Service Company, Bengaluru, India
E-Mail: srk1670@yahoo.com

ABSTRACT

C-arm systems are well established in clinical routines which produces two- dimensional (2D) projection images, which are not sufficient to provide the depth information required by surgeons during interventional procedures. Due to this, the procedural time and radiation dosage are significantly higher which leads to increased procedural cost. In order to extract depth information from 2D projection images acquired with stepwise rotation between0 to 180 degrees, various 3D volume construction algorithms are developed. The purpose of this paper is to systematically review the various 3D volume construction algorithms in order to develop a cost-effective solution to be incorporated in the iso-centric C-arm machines without 3D volume construction algorithms. The proposed review process is done in the following aspects: i. State-of-the-art 3D volume construction algorithms ii. Comparing the different aspects of commercially available iso-centric C-arm machines incorporated with 3D volume construction algorithms. The impact of various 3D construction algorithms in improving different aspects such as image quality, resolution, procedure time, radiation dose, and accuracy of the final 3D model is discussed. Based on the findings we recommend a procedure to develop and validate a 3D volume construction algorithm. 3D volume construction from C-arm images helps to construct Multi Planar Reconstruction (MPR) views during interventional procedures which will provide in-depth information and minimize the procedure time, cost, and dosage to the patient.

Keywords: 2D to 3D, MPR, fluoroscopy, interventional, radiology, visualization.

Manuscript Received 21 April 2023; Revised 15 October 2023; Published 27 October 2023

1. INTRODUCTION

The C-arm system provides real-time X-ray images, thus allowing the physician to monitor progress at any point during the surgery and helps to immediately make any corrections that may be required for various clinical applications (J.Moret *et al.* 1998; B.Unger *et al.* 1999; R.P.Kluecznik *et al.*1999) Mostly, C-arm devices are used in Cath lab procedures in the hospitals for visualizing and carrying out surgeries in cardiovascular regions, especially for viewing the vessels (A.C.Kak *et al.* 1977; R.A.Kuruger *et al.* 1987; W.J.T.Spyra 1990) Cath lab is a diagnosis room in a Hospital with imaging equipment which is involved in diagnosing and treating Cardio-vascular diseases. C-arm systems are used in various surgical and non-surgical procedures, especially in fluoroscopic intraoperative imaging in the areas of cardiology, orthopaedics, urology, neurovascular diseases, gastroenterology, etc. (Essam *et al.*). Some of the surgical procedures include abdominal and thoracic aortic aneurysm repair, percutaneous valve replacements, cardiac surgery, vascular surgery, bone implant replacement, traumatic conditions etc., whereas non-surgical procedures are the diagnosis of thrombus formation in vascular blood vessels using Digital Subtraction Angiography in cardiology, extracorporeal shockwave therapy during lithotripsy procedure in urology (Bush WH *et al.*1987), Road mapping and re-masking etc. Other applications include Thoracic, Lumbar and Sacral Pedicle Screw Placement, calcaneal fracture surgery, total knee arthroplasty, real-time tracking and navigation during procedures etc. (L.Adams *et al.* 1990; R.L Galloway 2001; C.A.Maruer *et al.* 1997; C.R Naruer *et al.* 1997; B.West *et al.* 2001; B.West *et al.* 2004; P.Grunet *et al.*2003)

Using the common interventional X-ray C-arm, only 2D projection images are produced, which are not enough to give the information required by surgeons. The most common challenge in using 2D images is that it is insufficient to provide information in complicated structures such as blood vessels, intestines, etc. For example, during surgery in a blood vessel using the C-arm, the catheter insertion is difficult as it may hit the walls of the vessels and lead to internal bleeding which may complicate the procedure in turn increase in procedural time. Similarly, the small intestine has many folds where the insertion of a catheter without any proper guidance may lead to tear any part of the folds or walls resulting in bleeding, which may lead to various problems for the surgeons as well as the patients. Thus, to avoid the above issues, 2D images captured using the C-arm are reconstructed into a three-dimensional (3D) volume which can be co-registered with the live fluoroscopic mode toget the depth view in real time. It can be viewed in Multiplanar Reconstruction (MPR) mode by the surgeons to carry out the interventional procedure effectively and quickly. But other problems can even arise due to a feeble number of projections and irregular placements of the C-arm due to mechanical instability of the systems. There are some flexible algorithms to handle irregular geometry using algebraic methods, A.Rougee *et al.* 1988 describe an overview and to handle inconsistent data, very sophisticated examples are described inE.Payot *et al.* 1997 & K.M. Andress *et al.* 1998.

C-arm systems are broadly categorized in to iso-centric and non iso-centric imaging. The 3D volume construction algorithms based on conventional X-ray projection imagesobtained by an iso-centric C-arm system have become more preferred approach since the images obtained are of high-resolution 2D projections, which are then being used for reconstructing 3D volume. Whereas, images reconstructed from non iso-centric projection provides lesser clarity and information than required, since the arm is being repositioned often to focus on the region that is to be imaged. On the other hand, modern day iso-centric C-arm systems are (inbuilt with advanced 3D volume construction algorithm and MPR visualization feature) called as 3D C-arm computed tomography. It uses 2D X-ray projectionsacquired with a Flat panel detector C-arm system to generate CT-like images. To this end, theC-arm system performs a sweep around the patient, acquiring up to several hundreds of 2D projection images. State of the art of various developed 3D volume construction algorithms such as the shift and add‘ algorithm, _Feldkamp‘ algorithm, _Feldkamp–Davis–Kress (FDK) reconstruction algorithm, _Cone beam reconstruction‘, _volume rendering‘ techniques, _fast back projection‘ methods (M.Ingerhed 1999, G.Lauritsch *et al*. 1998; H.Turbell *et al*. 1999),_Fourier‘ method (C.Jacobson 1999) and few others are analysed in the study. These algorithms overcome the limitations mentioned in the references (P.S.Cho *et al*. 1996; M.Li *et al*. 2002; V. Liu *et al*. 2003; J.Siewerdsen *et al*. 2005; G.H. Chen *et al*. 2006; S.Sorensen *et al*.2007; D.Ritter *et al*. 2007; E.A.Rasheed *et al*. 2012; X.Hun *et al*. 2012). The reconstruction of 3D images from a cone beam projection of the X-ray beam from the iso- centric C-arm provides orthogonal information such as sagittal, coronal plane and transverse. For example, Hagen *et al*. 2003 developed an algorithm for 3D rotational angiography of the transplant renal artery M.Grass *et al*. 1999 presented their 3D reconstructed models based on high-contrast objects, such as a vessel filled with contrast agent or bones obtained from a motorized C-arm system. These techniques also play a vital role in medical imaging and non-destructive testing (Rizo P *et al*. 1991; Cho PS *et al*. 1995; Wisent K *et al*. 1997; Johnson RH *et al*. 1997)

Though 3D C-arm computed tomography provides the required information but it lacks in fulfilling global needs as it is expensive and not commonly available. However, the existing iso-centric C-arm systems without 3D volume construction algorithm cannot be obsolete and a cost-effective solution to be provided to better usage of the system. The solution is to incorporate by adding 3D volume construction and MPR visualization features with the existing system. Hence, the present study focuses on the systematic review of state of the algorithms in respect of 3D volume construction from 2D projection images acquired with stepwise rotation of the C-arm between 0 degrees and 180 degrees; C-arm systems and recommends a constructive approach for a viable solution.

2. EVOLUTION OF C-ARM MACHINES

A C-arm is an imaging scanner intensifier. The name derives from the C-shaped arm which connects the X-ray source and X-ray detector with one another. C-arms have radiographic capabilities, though they are used primarily for fluoroscopic intra-operative imaging, thus allowing the physician to monitor the patient‘s progress and immediately make any corrections. Portable or mobile C-arm comprises a generator and a detector. The C-shaped connecting element allows movement horizontally, vertically and around the swivel axes, so that the X-ray images of the patient are produced from almost any angle that is required. The C-arm usually works in two modes, namely, the continuous mode and the pulsed mode. In the continuous mode, X-rays are exposed continuously whereas in the pulsed mode, X-rays are exposed when an image is required. Pulsed fluoroscopy reduced the fluoroscopy time by 76% and the radiation dose by 64% compared to continuous fluoroscopy. Based on the requirement, the mode is chosen during intervention procedures. C-arms consist of detectors such as image intensifiers or plat panel detectors. An Image intensifier converts X-rays into visible light at higher intensity than mere normal fluorescent screens do. X-ray imaging systems use such intensifiers (like fluoroscopes) that involve converting low-intensity X-rays to a bright visible light outputwhereas Flat panel detectors are involved in the conversion of X-rays to light or charge which is read out using thin film transistors. Nowadays, Flat-panel detectors (FDP) are increasingly replacing image intensifiers on mobile C-arm systems due to lower patient dose and increased image quality and no deterioration of the image quality over time.

Usually, the C-arm is designed as non iso-centric where the technician has to move the arm often to locate the centre point before imaging. So, in order to overcome this problem, iso-centric C-arms were developed which help the technicians to avoid the movement of the arm often. Once the arm is fixed, the centre point remains constant.

Other features that were developed over time include Smart Auto-Trak which automatically adjusts the image when anatomy is not focused at the centre, the Smart-Metal option which helps to maintain image resolution even after introducing metal objects in the X-ray field, the Smart Window to adjust the collimator position and automatically adjusts the window size for better image quality, Distance control, an assistance system implemented to support non- contact collision protection for patient‘s safety etc. Apart from the imaging facilities, the C- arm can even store images in the DICOM format for future use and transmit them to PACS stations if required.

As an advancement in C-arm technology, 3D C-arm computed tomography is a new and innovative imaging technique. It makes use of 2D X-ray projections acquired with an FDP C- arm system to generate CT-like 3D images, where the C-arm system performs a sweep around the patient, acquiring up to several hundred 2D views, which are given as input for 3D reconstruction

algorithms. The Resulting voxel data sets can be visualized either as cross-sectional images or as 3D data sets using different volume rendering techniques. In combination with 2D fluoroscopic or radiographic imaging, 3D C-arm imaging provides valuable information for therapy planning, guidance, and outcome assessment, all in the interventional suite. This option is especially found only in certain C- arms such as Ziehm Vision RFD and Arcadis Orbic 3D. Further, the algorithms used to construct 3D projections from 2D ones are given below.

3. RECONSTRUCTION ALGORITHMS

3.1 Shift and Add Method

The Shift-and-Add algorithm approach plays an important role in 3D reconstruction and is broadly used in tomosynthesis and overlapped complicated structures, such as joints, etc (Senhu Li *et al*. 2005). This method makes use of a principle, in which acquired images are lined up and the algorithm is applied by shifting and adding the projected images. Senhu Li *et al* with the base of this algorithm, developed 3D projections explained by Z. Kolitsi *et al*. 1992 to reconstruct the tomographic images. Image acquisition is done by taking the total N_t in certain angle Θ at constant increment; For example, in this method, An OEC® Miniview 6800 Mobile C-arm system (GE Medical System) was used to acquire projected images. A phantom consisting of two dry chicken bones was used to test the reconstruction algorithm. This algorithm results in low contrast reconstructed image with a blurred background. In order to remove the blurred background, the segmentation concept is used. The general workflow is shown in Figure-1.

These outputs are obtained by shifting and adding the projection images obtained at an even shifting of the mobile C-arm. On comparing the reconstruction results in this study, the 3D reconstructed model reduces the error by 10% by measuring the maximum thickness of the bone. Thus, using the shift-and-add algorithm, the structures in the reconstructed tomographic images are more accurate and the image intensity values are distinguishable with respect to the background and objects. This method overcomes the image truncation problem which was found in the back-projection method resulting in a simple and practical method for reconstruction [38].

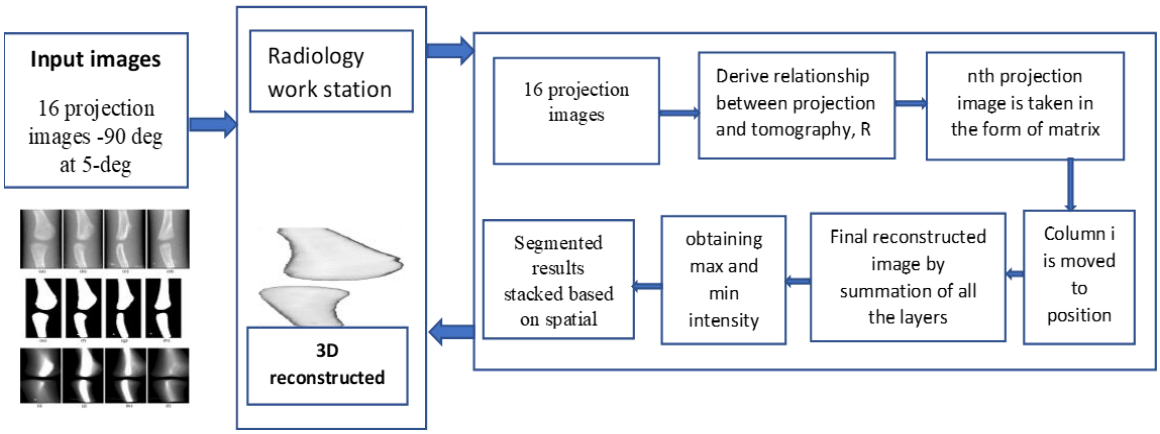

Figure-1. Workflow of the shift and add reconstruction method.

Table-1. Review of different types of C-arm devices and its imaging features.

Various types of C-arm available are:				
Model name	**Features**	**Detector andDisplay**	**Storage options**	**Applications**
GE HEALTH CARE				
OEC Brivoprime C- arm	Smart Auto Trak SmartMetal Smart Window Arm rotation: 410° radial rotation,120°orbital rotation, 25°wigwag No specific value ofm A and kVp(40-110)…Auto brightness stabilization- automatically adjustvalues to obtain better images at low dose.	Image intensifier-converts X-ray intovisible light and amplifies the output obtained. LCD high-resolution monitor	CD, DVD, or USB save optionsare available andstored in BMP, MPPS, and DICOM format. BMP-Bitmap-type of format tostore digital image. DICOM- is a standard use to store and transmit medical images.	Help to differentiate soft tissue organs and anatomy in the image field.
OEC 9900 Elite	Motion tolerantsubtraction Autotrak 3.SmartMetal 4. Smart window 5.Lateral, orbital orombination movement 6.120 kVp and 75 mAfor radiographicxposure. 7. Continuous highlevel fluoro up to 20mA. 8. Pulsed fluorographymode up to 40 mA.9. Automatic Brightness Stabilization	1.Image intensifier 2.Flat panel detectors	1.CD/DVD, USB memoryoptions and stored in DICOM format	Used in urology, endoscopy, orthopedics, vascular and other emergency procedures.
SIEMENS				
Cios Alpha	Digital Subtraction Angiography Retina 3D scan technology smart collimation 4.oribital movement-	CMOS (complementary metal oxide semiconductor) flatdetector High-contrast TFT-	1.CD/DVD, USB and DVD recording. DICOM 3.0 format is used.	vascular and cardiac surgery, astroenterology, urology, traumaand spine surgery

3.2 Feldkamp Algorithm

Feldkamp's method is applied over the 2D projections obtained with the C-arm systems measured along a circular type of source-detector trajectories. In order to reconstruct the images accurately, the system trajectories should be known. The position of the focal spot and of the detector should be measured to determine the system trajectories (Koppe R *et al*. 1995; Koppe R *et al*. 1996; Fahrig R *et al*. 1997)) 2D images are acquired by either single or double half circular trajectories. This algorithm was widely used in the area of medical imaging and non-destructive testing. The adaptation of this method is used in the 3D reconstruction of 2D projected images of a vessel with a contrast agent and of a bone. In this method, the standard Philips INTEGRIS BV3000 C-arm system was used to acquire images in both single and double half circular trajectories. Feldkamp algorithm used in the 3D reconstruction is shown in the form of a flow diagram in Figure-2. The resulting method is a simple and straightforward approach to reconstruct the 2D projections. Several errors occur while adopting this method due to the missing data problem as a result of the incomplete source-detector movement as explained in tuy's condition (Tuy HK 1983; Smith BD 1985). Another error that may occur if the cone size is smaller than the object size is the truncated projection problem, which often occurs in medical applications. The Feldkamp method is applied to the required region of interest and results in a high-contrast 3D object with an isotropic spatial resolution with respect to the background. For example, consider 100 2D projections of the cervical vertebra column acquired as mask images to be used in digital subtraction angiography (DSA) shown in Figure-3, which are reconstructed as a 3D object. The output of this algorithm is a reconstructed 128^3 3D data set of the cervical vertebral column shown in Figure-4. Similarly, consider 100 projections of a 2D projection of blood vessel with iodine contrast injected for every image captured, where images with no contrast are ejected during the reconstruction process. The 2D projections are acquired by double half-circular trajectory covering 180 degrees as shown in Figure-5. The reconstructed 3D resultsof a blood vessel with a contrast agent are shown in Figure-6. Thus, the Feldkamp method results in high contrast 3D objects with respect to the background of the acquired projections.This study also resulted in less error in double half-circular trajectory image acquisition than the single half-circular trajectory image acquisition.

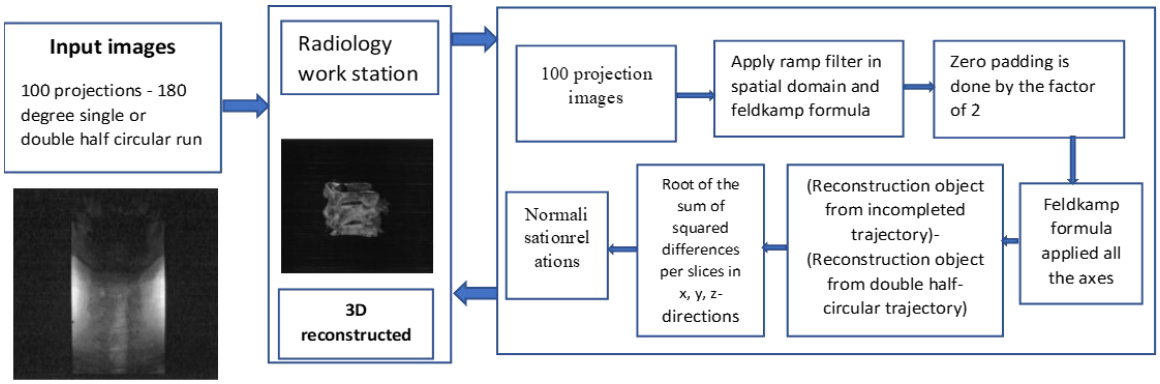

Figure-2. Workflow of the Feldkamp method.

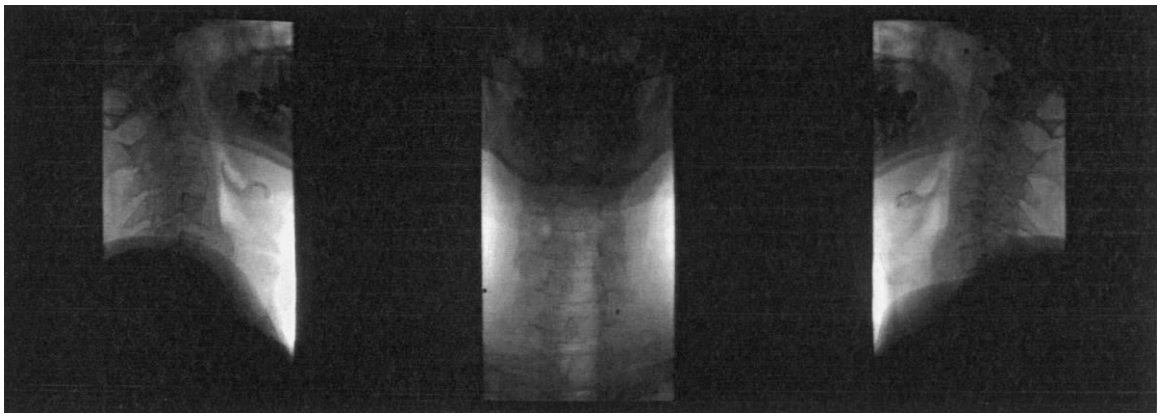

Figure-3. Three different 2D projections of a subject's cervical spine measured with animage intensifier during a half-circular trajectory.

Figure-4. Three different views of a volume-rendered reconstructed 3D data set of a cervicalvertebra column.

Figure-5. Three different cone–beam projections of a cerebral vessel tree filled with contrastagent measured with an image intensifier during a double half circular rotational run.

Figure-6. Three different views of a volume-rendered reconstructed 3D rotationalangiography data set.

3.3 M-Line Method

The M-line method is an image reconstruction method which is carried out in the filtered back projection mode. The main aim of this method is to implement an accurate filtered back projection algorithm for the 2D projections obtained from a c-arm system without moving the patient‘s table: i.e. circle-plus-arc trajectory which avoids error data acquisition geometry and requires no ideal filtering step, even if the geometry is non-ideal (Stefan Hoppe *et al*. 2012) The M-line method adopted in this procedure *was* originally presented by Pack J *et al*., 2005 for 3D reconstruction. Data acquisition was carried out using an Artis zee ceiling-mounted C-arm system (SiemensAG, Healthcare Sector, Forchheim, Germany) where the source and detector is moved over the region of interest in a circle-plus- arc trajectory (D.L.Donoho 2006). An anthropomorphic thorax phantom was used to acquire 597 2D projections for reconstruction. The M-line algorithm is shown in the form of a flow diagram in Figure-7. The results of the M-line algorithm are compared with those of the Feldkamp method where the truncation problem is reduced. The error due to data acquisition in the Feldkamp method is rectified in the M-line algorithm. This method also avoids discretization errors that out-weighed the benefits of the cone-beam artefacts mitigation. Through, projections, it provides more accurate and detailed information than the Feldkamp method, which has already been explained.

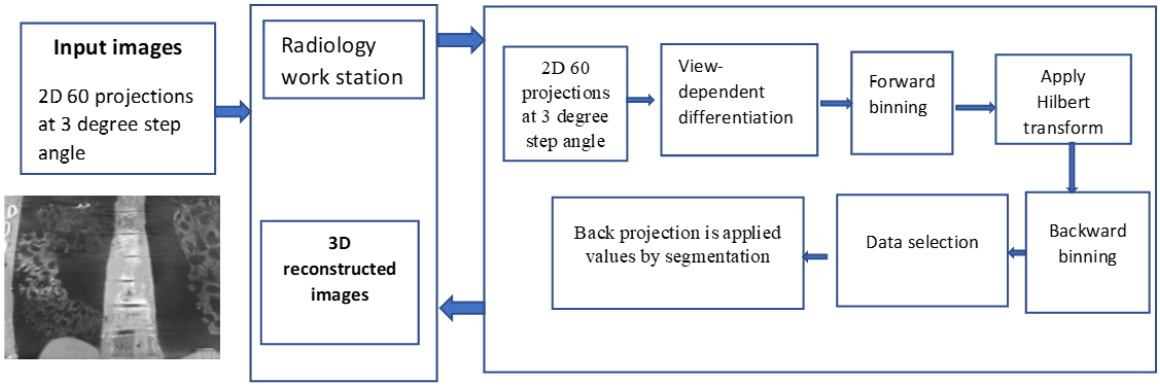

Figure-7. Workflow of the M-Line method.

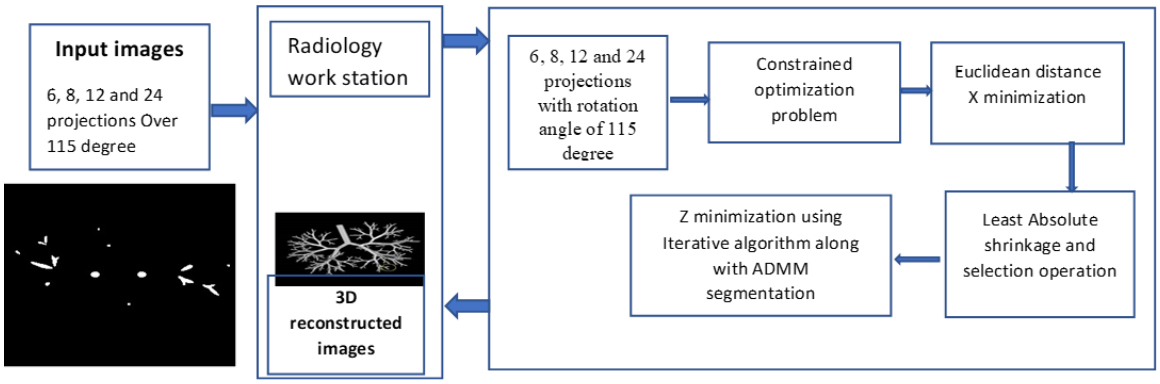

Figure-8. Workflow of the SCAN method.

3.4 Sparsity-Constrained Angiography (SCAN) Iterative Algorithm

Sparsity-constrained angiography is derived using the Alternating Direction Method of Multipliers which emphasises on the sparse nature of angiography imaging. The proposed algorithm is based on the theory of Compressed Sensing (CS) (E.J. Can des *et al*. 2006; Grass M *et al*. 1999) where image reconstruction is carried out by introducing a sparsity-constrained cost function. The image reconstruction algorithm was developed to handle sparse objects such as blood-vessels, where most of the image pixel values are close to zeros or zero and only a feeble number of image pixels have non-zeros intensities. The 2D projections used in 3D reconstruction are obtained using the clinical C-arm scanner (Ziehm Vision R, Ziehm Imaging GmbH, Nurnberg, Germany) with an orbital movement of 115 degrees.

The phantom was designed to represent lung bronchial airways. The 2D projections were obtained with a rotation angle spacing of 20, 15, 10 and 5 degrees with 6, 12, 18 and 24 projections respectively. Then, the SCAN Algorithm was applied, as shown in Figure-8. Thus, the proposed algorithm was designed to overcome data limitation problems, such as limited views, short orbit and offset scan geometries in this imaging modality. The benefits ofthis algorithm are that it resulted in 3D images (Figure-9) using conventional inexpensive equipment and it improved the image quality which was obtained from highly down-sampled projection data. The only error caused is due to the gantry mechanical rotation and it is required to perform system calibration for high-quality 3D reconstructed images.

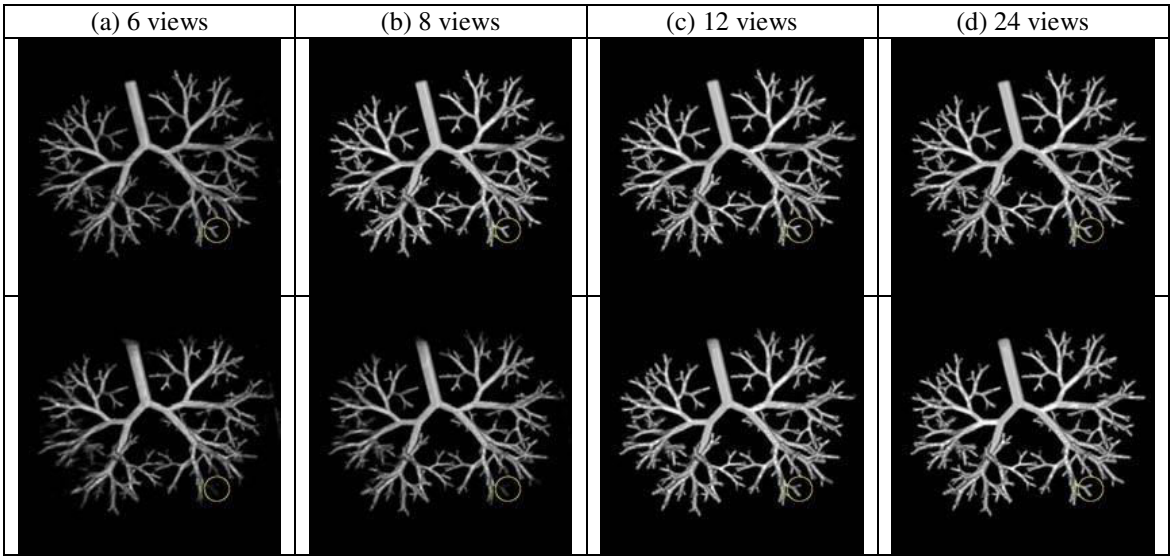

Figure-9. Three-dimensional volume rendering of SCAN reconstruction with differentprojection views.

3.5 Cone Beam Reconstruction Algorithm

C-arm based cone-beam CTs are a widely used imaging modality during intraoperative procedure. Typically, a C-arm CT scan is nowadays performed using a circular or elliptical trajectory around a region of interest (Figures 10, and 11). The benefits of an intra-operative C-arm cone-beam computed tomography (CBCT) with a flat-panel detector (FPD), are that it offers sub-mm spatial resolution and soft-tissue visibility at low radiation. The proposed trajectory method in this work extends the use of the mechanical rotation range of the C-arm system with two additional linear shifts of the X-ray tube and detector

to increase the angular sampling range within the required field of measurement (FOM) [20]. Other implementations of C-arm-based cone-beam reconstruction techniques also exist (G.Lauritsch *et al*. 1998; Riddell C *et al*.2006). The mobile C-arm systems (Ziehm RFD 3D, Ziehm Imaging, Nurnberg, Germany) were used to acquire datasets using a living pig and a cadaver with the angle of 164.5◦ rotation for taking a complete data set using the rotate-plus-shift trajectory.

The path trajectory of the C-arm consists of circular or elliptical rotation of the C around a defined isocentric point and two linear translations travel parallel to the detector plane at the beginning and at the end of the scan, respectively. Combining all these three parts to one trajectory enables the acquisition of a sampled data set using only 180◦ minus (164.5 degree) fan angle of rotation. The head of the live pig is placed in the dorsal position on an X-ray imaging patient‘s bed and scanning was done in both the short scan and the rotate-plus-shift trajectory. The short scan and the rotate plus-shift scan were acquired using 512 projections (with the time of 41 sec per scan), the 165◦ limited angle scan using 431 projections (about 35 s). To reconstruct 3D images, the SART Algorithm (Figure-12) along with a filtered back projection was used (K.Wisent *et al*. 2000; F.Noo *et al*. 2002). The rotate-plus-shift trajectory when combined with the reconstruction algorithms helps to avoid limited angle artefacts (E.Y.Sidky *et al*. 2006; L.Ritschi *et al*. 2011; M.Y.Wang *et al*.1996).

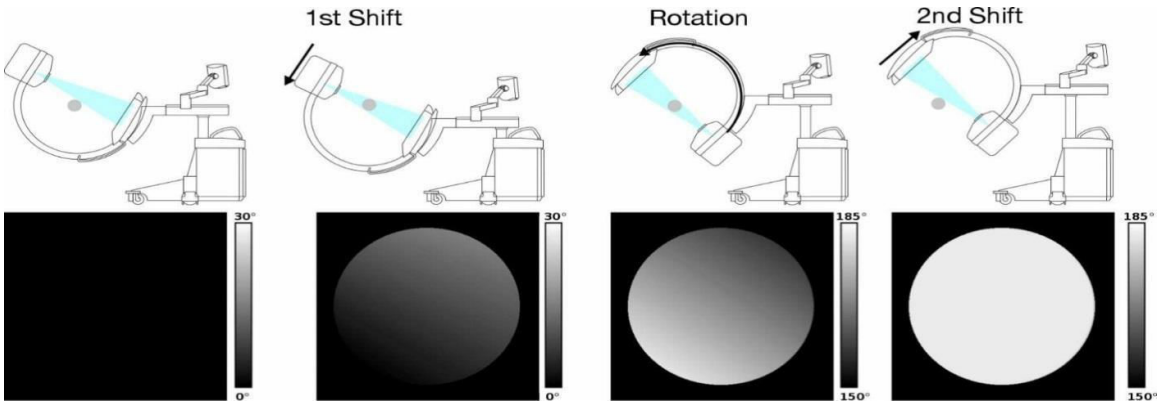

Figure-10. The rotate-plus-shift trajectory illustrated in four positions of a C-arm used in this study.

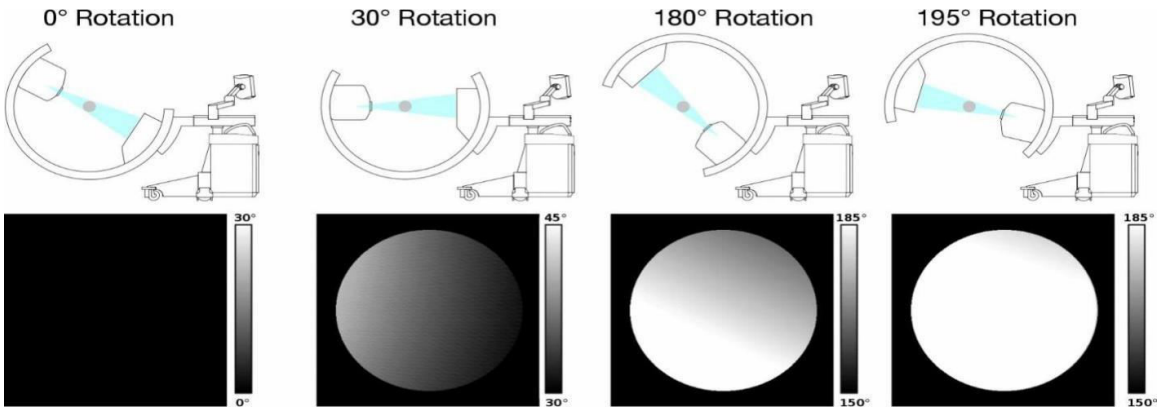

Figure-11. Data acquisition at regular intervals.

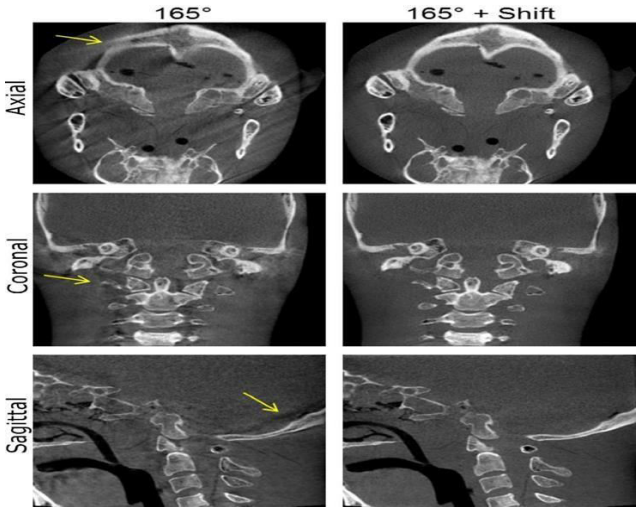

Figure-12. Reconstruction of the anthropomorphic head phantom was acquired with 165◦ and 165◦+ shift. Thus, the proposed trajectory method allows for the acquisition of data samples with a mobile C-arm system which has mechanical rotation limited to a range of at least 180◦ minus. Therefore, the rotate-plus-shift method helps to integrate full 3D functionality into the mobile C-arm devices to avoid any loss due to handling and usability for 2D imaging. This is mainly used in intraoperative 3D imaging in a wide range of clinicalapplications.

4. DISCUSSIONS

This review presents a detailed survey of algorithms involved in the 3D reconstruction of 2D projections obtained from the degree wise rotation of the C-arm at various angles. 3D reconstructed images will help the surgeons to locate the area accurately in reconstructed 3D projections which provide high integrity in carrying out the surgeries effectively and to obtainbetter results, once the surgery is completed.

This 3D reconstructed view plays a major role in various applications like surgeries in blood vessels, Thoracic Screw Placement, Lumbar Screw Placement, Sacral Pedicle Screw Placement, calcaneal fracture surgery etc. In the case of blood vessel imaging, 2D images are insufficient to provide the required 3D information of vessel anatomy due to its complicated structure and the inability to identify overlapping vessels (E.J.Cand es *et al*. 2006). Hence, the 3D reconstructed images help to overcome the above problem in the case of blood vessels. The reconstructed images obtained in the case of locating a kidney help in pointing out stones for lithotripsy treatment (Bush WH *et al*. 1997). Computer-assisted virtual neuro-navigation improves the precision of Pedicle screw placement and minimization of surgical procedures while using 3D reconstructed images (Gonzalvo A *et al*. 2009). The reconstructed images also help to assess the successful aneurysm exclusion in fenestrated branched endovascular aneurysm repair using C-arm cone-beam computed tomography (Dijkstra ML *et al*. 2010), and this involves treating the aneurysm repair effectively by locating the area accurately. Rotational angiography with digital 3D reconstruction allows to carry out per- procedural 3D imaging to facilitate cardiac ablation procedures during cardiac surgery. Using, single C-arm rotation per-procedural 3D imaging of the atria and ventricles can be done with a lower contrast and radiation dose (K.Atesok a *et al*. 2007). An intraoperative C- arm X-ray device with 3D imaging capabilities (3D rotational X-ray (3DRX)) coupled withan image guided navigation system with 3D imaging capabilities (3DRX) enables direct navigation without invasive image-to-patient registration on 3DRX volumes for evaluation before surgery is carried out (Everine B *et al*. 2006). This approach allows multiple navigation based on intraoperative procedure acquired 3D fluoroscopic images (Foley *et al*., 2001; Fritsch *et al*., 2002; Hofstetter *et al*., 1999; Nolte *et al*., 2000). The other applications include isocentric 3D C-arm Intraoperative visualisation for fracture reduction and implant positioning in orthopaedic trauma surgery. Intraoperative reconstructed 3D visualisation of intraarticular fractures enables the surgeon to identify improper implant positions and hence may eliminate the need for re-do procedures (K.Atesok a *et al*. 2007). Richter *et al* identified an unacceptable reduction or implant malposition in 39% While imaging, using C-arm at an isocentric position (Richter M *et al*. 2005). Three-dimensional reconstructed images also playa vital role in total knee arthroplasty, with ISO-C imaging, it helps to measure rotational alignment in knee arthroplasty with high accuracy and repeatability comparable with CT imaging modality. Isocentric imaging using the C-arm has potential as an intraoperative tool to accurately align arthroplasty components during abnormal conditions either due to accidents or disease (Shahram Amiri *et al*. 2013; Takahito *et al*.2013). C-arm reconstructed images also play a vital role in various applications for detecting screw misplacement and in decreasing the rate of revision surgery for screw misplacement with high Reliability and accuracy (Praveen Satarasinghe *et al*. 2012; Helalis I.D *et al*. 2012).

Thoracic, Lumbar, and Sacral Pedicle Screw Placement was carried out using Ziehm vision RFD 3D and Navigated Stryker Cordless Driver3. 3D imaging for computer-assisted virtual neuro-navigation improves the precision of Pedicle screw placement and minimization of surgical procedures. This algorithm helps to overcome certain disadvantages, such as screw positioning, visualization of a pedicle‘s trajectory, radiation exposure, increased time expenditure, and possible workflow interruption. Human Vagus Nerve Branching in the Cervical Region which was so complicated has become easy with the help of Ziehm vision RFD 3D. It helped in locating the Metal needles in the cranial and caudal part that was visibleof the CVN and CVN branches from the cervical region in the anterior-posterior and lateral projections [63]. Investigation of first ray mobility during gait by kinematic fluoroscopic imaging in the plantar/dorsal flexion in the sagittal plane was performed using Ziehm. This procedure using Ziehm vision RFD 3D is used to find out the quantification of the in-vivo sagittal mobility of the joints of the medial foot column during the roll-over process underfull weight bearing (Shahram

Amiri *et al*. 2013). This overcame problems associated withskin motion and the adjacent structures which reduce the resolution and anatomical discrimination without making use of any invasive methods (Praveen Satarasinghe *et al*. 2012; Helalis I.D *et al*. 2012). These are some of the problems solved using the Ziehm vision RFD 3D C-arm machine. It increases the accuracy and resolution of imaging the anatomical structures during intraoperative procedures and in various other complicated surgical applications.

Arcadis orbic were used to place 446 pedicle screws into 100 patients. The demographics of the patients include 15 cases of scoliosis, 36 cases of spondylolisthesis, and 21 cases of revision surgery. The location of pedicle screw placement was 12 thoracic, 352 lumbar, and 82 sacral screws (Gonzalvo A *et al*. 2009) which were carried out successfully. This machine helps to overcome neurologic deficits after pedicle screw surgery which is reported to occur up to 5% of the time (Zhao X *et al*. 2016; Lee M.H *et al*. 2013) and misplaced pedicle screw rates with traditional techniques which have been reported to be 10-42% (Kim YJ *et al*. 2004;Hammer N *et al*. 2015; Heiner Martin *et al*. 2012; Nester CJ *et al*. 2007; Nester CJ *et al*. 2007; Lundgren P *et al*. 2008; Robert Green Watkins *et al*. 2010). All these above complications were overcome by the usage of the Arcadis orbic 3D C-arm. Arcadis orbic 3D fluoroscopy was performed on some patients after they were extensively evaluated by 2D fluoroscopy during surgery to compare the results of both. In conventional calcaneal fracture surgery, surgeons evaluate that misplacements of implants take place while using 2D fluoroscopy. Also, 2D fluoroscopy cannot completely find or locate the complex anatomy of the calcaneus. Therefore, if the image obtained by 2D fluoroscopy is unclear and has less resolution (Esses SI *et al*. 1993), intraoperative 3D fluoroscopy using Arcadis orbic 3D was used (Wang JC *et al*. 2005; Castro W *et al*. 1996; Farber GL *et al*. 1995).

Surgery in patients with hip fractures has increased with the large demographic growth of geriatric patients in the present world (Gertzbein SD *et al*. 1990). For those patients, exact screw placement with a greater distance between the screws enables a biomechanically stable fixation but this has become very challenging. So, to overcome the above problem, Mobile C-arms with 3D imaging were used for intraoperative 3D visualisation of the anatomical areas. The Iso-C 3D mobile C-arm has equal clinical value to spiral computed tomography which is used widely in various surgical procedures. Hence, 3D computer-assisted navigation helps to reduce the number of drilling attempts during the operations and the operating time while optimising the precision of hip screw placement compared to the conventional fluoroscopy-based technique (Guven O *et al*. 1994). Arcadis orbic plays a significant role in imaging the anatomical structures during the intraoperative procedures and obtaining a volume rendered image for more accuracy and better resolution ofthe structures that are imaged.

CONCLUSIONS

There are many algorithms in the literature describes about the construction of 3D volume from 2D projection images acquired with step wise rotation of isocentric C-arm. These algorithms were evaluated against corresponding CT image volumes and were produced good accuracy of the constructed volumes. This 3D volume construction helps to construct Multi Planar Reconstruction (MPR) views during interventional procedures which will provide in- depth information and to minimize the procedure time, cost and dosage to the patient.

Conflict of Interest:

All authors declare that there is no conflict of interest related to this article. No funding received for this study. No human / animal samples involved in this study. Hence, no ethical clearance is required.

REFERENCES

Essam A. Rashed, Mohammad al-Shatouri, Hiroyuki Kudo. Sparsity-constrained three-dimensional image reconstruction for C-arm angiography, Computers in Biology and Medicine, PII: S0010- 4825(15) 00132-8.

J. Moret, R. Kemkers, J. Op de Beek, R. Koppe, E. Klotz, and M. Grass. 1998. 3D rotational angiography: clinical value in endovascular treatment, Medica Mundi. 42(3): 8-14.

B. Unger, J. Link, J. Trenkler and H. Böhm-Jurkovic. 1999. Digital 3D rotational angiography in preoperative and preinterventional diagnosis of intracranial aneurysms, ‖ RöFo, pp. 482–491. (full paper in German only).

R. P. Klucznik and M. E. Mawad. 1999. Utilization of three-dimensional rotational angiography in the evaluation and endovascular treatment of cerebral aneurysms and arteriovenous malformations, ‖ RSNA 99, Supplement to Radiology. 213: 276.

A. C. Kak, C. V. Jakowatz N. A. Baily, and R. A. Keller. 1977. Computerized tomography using video recorded fluoroscopic images, ‖ IEEE Trans. Biomed. Eng. 24: 157-169.

R. A. Kruger, D. R. Reinecke, S. W. Smith and R. Ning. 1987. Reconstruction of blood vessels from x-ray subtraction projections: limited angle tomography,‖ Med. Phys. 14(6): 940-949.

W. J. T. Spyra, A. Faridani, K. T. Smith and E. L. Ritman. 1990. Computed tomographic imaging of the coronary arterial tree-use of local tomography,‖ IEEE Trans. Med. Imag. 9: 1-4.

Bush W. H., Brannen G. E. 1987. ―Extracorporeal shock-wave lithotripsy (ESWL) of pelvic kidney calculus. Use of C-arm fluoroscopy for correct patient positioning‖, medline. 29(4): 357-60.

L. Adams, W. Krybus, D. Meyer-Ebrecht, R. Ruege, J. M. Gilsbach, R. Moesges and G. Schloendorff. 1990. Computer-assisted surery, ‖ IEEE Comput. Graphics Appl. 10: 43-51.

R. L. Galloway Jr. 2001. The process and development of image-guided procedures,‖ Annu. Rev. Biomed. Eng. 3: 83-108.

C. R. Maurer, Jr., J. M. Fitzpatrick, M. Y. Wang, R. L. Galloway. , Jr., R. J. Maciunas and G. S. Allen. 1997. Registration of head volume images using implantable fiducial markers,‖ IEEE Trans. Med. Imaging. 16: 447-462.

J. B. West, J. M. Fitzpatrick, S. A. Toms, C. R. Maurer Jr. and R. J. Maciunas. 2001. Fiducial point placement and the accuracy of point-based, rigid body registration,‖ Neurosurgery. 48: 810-816.

J.B. West and C. R. Maurer, Jr. 2004. Designing optically tracked instruments for image-guided surgery,‖ IEEE Trans. Med. Imaging. 23: 533-545.

P. Grunet, K. Darabi, J. Espinosa and R. Filippi. 2003. Computer-aided navigation in neurosurgery, ‖ Neurosurg. Rev. 36: 73-99.

A. Rougée, K. M. Hanson and D. Saint-Felix. 1988. Comparison of 3D-tomographic algorithms for vascular reconstruction, ‖ SPIE, vol. 914, Medical Imaging II, pp. 397-405.

E. Payot, F. J. Preteux, Y. Trousset, and R. Guillemaud. 1997. Generalized support constraint for three-dimensional reconstruction from incomplete Fourier spectra,‖ J. Electron. Imag. 6(4): 426-438.

K. M. Andress. 1998. Evidential reconstruction of vessel trees from rotational angiograms,‖ in IEEE Int. Conf. Image Process., Los Alamitos, CA. pp. 385-389.

M. Ingerhed. 1999. Fast backprojection for computed tomography,‖ dissertation, Univ Linköping.

G. Lauritsch and W. Härer. 1998. A theoretical framework for filtered backprojection in tomosynthesis,‖ SPIE, vol. 3338, Conf. Image Process. pp. 1127-1137.

H. Turbell and P. Danielsson, —Fast Feldkamp reconstruction,‖ in Proc. 1999 Int. Mtg. Fully Three-Dimensional Image Reconstruct. Radiol. Nuclear Med., Egmond aan Zee. pp. 311-314.

C. Jacobson. 1996. Fourier methods in 3D-reconstruction from cone-beamdata,‖ Linköping Studies in Science and Technology Dissertations No. 427.

P. S. Cho, A. D. Rudd, R. H. Johnson. 1996. Cone-beam CT from widthtruncated projections, Computerized Medical Imaging and Graphics. 20, 49(57).

M. Li, H. Yang, H. Kudo. 2002. An accurate iterative reconstruction algorithm for sparse objects: application to 3D blood vessel reconstruction from a limited number of projections, Physics in Medicine and Biology. 47, 2599{2609.

V. Liu, N. R. Lariviere, G. Wang. 2003. X-ray micro-CT with a displaced detector array: Application to helical cone-beam reconstruction, Medical physics. 30, 2758{2761.

J. Siewerdsen, D. Moseley, S. Burch, S. Bisland, A. Bogaards, B. Wilson, D. Ja_ray. 2005. Volume CT with a at-panel detector on a mobile, isocentric C-arm: pre-clinical investigation in guidance of minimally invasive surgery, Medical physics. 32, 241{254.

G. H. Chen, J. Zambelli, B. E. Nett, M. Supanich, C. Riddell, B. Belanger, C. A. Mistretta. 2006. Design and development of C-arm based cone-24 beam CT for image-guided interventions: initial results, in: Proc. SPI 6142, Medical Imaging: Physics of Medical Imaging, p. 614210.

S. Sorensen M., Mitschke T. 2007. Solberg, Cone-beam CT using a mobile C-arm: a registration solution for IGRT with an optical tracking system, Physics in Medicine and Biology. 52, 3389{3404.

D. Ritter, J. Orman, C. Schmidgunst, R. Graumann. 2007. 3D soft tissue imaging with a mobile C-arm, Computerized Medical Imaging and Graphics. 31, 91-102.

E. A. Rashed, H. Kudo. 2012. Statistical image reconstruction from limited projection data with intensity priors, Physics in Medicine and Biology. 57, 2039{2061).

X. Han, J. Bian, E. L. Ritman, E. Y. Sidky, X. Pan. 2012. Optimization-based reconstruction of sparse images from few-view projections, Physics in Medicine and Biology. 57, 5245(5273).

G. Hagen, J. Wadstrom and A. Magnusson. 2003. —3D rotational angiography of transplant kidneys,‖ Acta Radiol. 44, 193-198.

M. Grass et al. 1999. Three-dimensional reconstruction of high contrast objects using C-arm image intensifier projection data, ‖ Comput. Med. Imaging Graph. 23, 311-321.

Rizo P, Grangeat P, Sire P, Lemasson P, Melennec P. 1991. Comparison of two three-dimensional X-ray cone-beam reconstruction algorithms with circular source trajectories. J Opt Soc Am A. 8(10): 1639-48.

Cho P. S., Johnson R. H., Griffin T. W. 1995. Cone-beam CT for radiotherapy applications. Phys Med Biol. 40: 1863-83.

Wisent K., Graumann R., Fahrig R., Holdsworth DW, Fox AJ, Navab N., Bani-Hashemi A. 1997. 3D- reconstruction during interventional neurological procedures. International Meeting on Fully Three- dimensional Image Reconstruction in Radiology and Nuclear Medicine. Nemacolin Woodlands.

Johnson R. H., Hu H., Haworth S. T. 1997. Circular and circle-and-line orbits for cone-beam X-ray microtomography of vascular networks. International Meeting on Fully Three-dimensional Image Reconstruction in Radiology and Nuclear Medicine. Nemacolin Woodlands.

Senhu Li and Huabei Jiang. 2005. A practical method for three-dimensional reconstruction of joints using a C-arm system and shift-and-add algorithm, Medical Physics. 32, 1491.

Z. Kolitsi, G. Panayiotakis, V. Anastassopoulos, A. Scodra, and N. Pallikarakis. 1992. A multiple projection method for digital tomosynthesis,‖ Med.Phys. 19, 1045-1050.

Koppe R., Klotz E., Op de Beek J., Aerts H. 1995. 3D vessel reconstruction based on rotational angiography. Proceedings CAR‘95. Berlin.

Koppe R., Klotz E., Op de Beek J., Aerts H. Digital stereotaxy/stereotactic procedures with C-arm based rotation-angiography. Proceedings CAR‘96. Paris, 1996.

Fahrig R., Moreau M., Holdsworth D. W. 1997. Three-dimensional computed tomography reconstruction using a C-arm mounted XRII: correction of image intensifier distortion. Med Phys. 24(7): 1097-106.

Tuy H. K. 1983. An inversion formula for cone–beam reconstruction. SIAM J Appl Math. 43(3): 546-52.

Smith BD. 1985. Image reconstruction from cone-beam projections: necessary and sufficient conditions and reconstruction methods. IEEE Trans Med Im. MI-4(1): 14-25.

Stefan Hoppe, Joachim Hornegger, Frank Dennerlein, Günter Lauritsch Frédéric Noo. 2012. Accurate image reconstruction using real C-arm data from a Circle-plus-arc trajectory‖, Int J CARS. 7: 73- 86.

Pack J., Noo F. 2005. Cone-beam reconstruction using 1d filtering along the projection of m-lines. Inverse Probl. 21(3): 1105-1120.

D. L. Donoho. 2006. Compressed sensing, IEEE Transactions on Information Theory. 52: 1289-1306.

E. J. Cand`es, J. Romberg, T. Tao. 2006. Robust uncertainty principles: Exact signal reconstruction from highly incomplete frequency information, IEEE Transactions on Information Theory. 52: 489-509.

Grass M., Koppe R., Klotz E., Proksa R., Kuhn M. H., Aerts H., Op De Beek J., Kemkers R. 1999. Three-dimensional reconstruction of high contrast objects using c-arm image intensifier projection data. Comput Med Imaging Graph. 23: 311-321

G. Lauritsch and W. Härer. 1998. A theoretical framework for filtered backprojection in tomosynthesis,‖ SPIE, vol. 3338, Conf. Image Process. pp. 1127-1137.

Riddell C., Trousset Y. 2006. Rectification for cone-beam projection and backprojection. IEEE TransMed Imaging. 25(7): 950-962.

K. Wiesent, K. Barth, N. Navab, P. Durlak, T. Brunner, O. Schuetz and W. Seissler. 2000. Enhanced 3-D-reconstruction algorithm for C-arm systems suitable for interventional procedures,‖ IEEE Trans. Med. Imaging. 19, 391-403.

F. Noo, M. Defrise, R. Clackdoyle, and H. Kudo. 2002. Image reconstruction from fan-beam projections on less than a short scan,‖ Phys. Med. Biol. 47, 2525-2546.

E. Y. Sidky, C. Kao, and X. Pan. 2006. Accurate image reconstruction from fewviews and limited-angle data in divergent-beam CT,‖ J. X-Ray Sci. Technol. 14, 119-139.

L. Ritschl, F. Bergner, C. Fleischmann and M. Kachelrieß. 2011. Improved total variation-based CT image reconstruction applied to clinical data,‖ Phys. Med. Biol. 56, 1545-1561.

M. Y. Wang, C. R. Maurer, Jr., and J. M. Fitzpatrick. 1996. An automatic technique for finding and localizing externally attached markers in CT and MR volume images of the head,‖ IEEE Trans. Biomed. Eng. 43: 627-637.

Bush W. H., Brannen G. E., ―Extracorporeal shock-wave lithotripsy (ESWL) of pelvic kidney calculus. Use of C-arm fluoroscopy for correct patient positioning‖, medline, 1987 Apr; 29(4):357-60.

Dijkstra M. L., Eagleton M. J., Greenberg R. K., Mastracci T., Hernandez A. 2011. Intraoperative C-arm cone- beam computed tomography in fenestrated/branched aorticendo grafting―, J Vasc Surg. 53(3): 583-90. Epub 2010 Dec 3.

Ector J., De Buck S., Nuyens D., Rossenbacker T., Huybrechts W., Gopal R., Maes F., Heidbüchel H. 2009. Adenosine-induced ventricular asystole or rapid ventricular pacing to enhance three-dimensional rotational imaging during cardiac ablation procedures‖, Europace. 11(6): 751-62.

Everine B. van de Kraats a, Theo van Walsum, Lance Kendrick, Niels J. Noordhoek, Wiro J. Niessen. 2006. Accuracy evaluation of direct navigation with an isocentric 3D rotational X-ray system‖, Medical Image Analysis. 10: 113-124.

K. Atesok a, J. Finkelstein b, A. Khoury a, A. Peyser a, Y. Weil a, M. Liebergall a, R. Mosheiff a. 2007. The use of intraoperative three-dimensional imaging (ISO-C-3D) in fixation of intraarticular fractures‖, Injury, Int. J. Care Injured. 38, 1163-1169.

Richter M., Geerling J., Zech S., et al. 2005. Intraoperative three-dimensional imaging with a motorized mobile C-arm (SIREMOBIL ISO-C-3D) in foot and ankle trauma care. A preliminary report. J Orthop Trauma. 19: 259-66.

Shahram Amiri, PhD, David R. Wilson, PhD, Carolyn Anglin, PhD, Andrew Van Houwelingen, MD and Bassam A. 2013. Masri, MD*, ―Isocentric 3-Dimensional C-Arm Imaging of Component Alignments in Total Knee Arthroplasty with Potential Intraoperative and Postoperative Applications‖, The Journal of Arthroplasty. 28(2).

Takahito Fujimori, MD, PhD, Motoki Iwasaki, MD, PhD, Yukitaka Nagamoto, MD, PhD Masafumi Kashii, MD, PhD, Masaki Takao, MD, PhD, Tsuyoshi Sugiura MD and Hideki Yoshikawa. 2013. MD, PhD,‖ Reliability and usefulness of intraoperative three-dimensional imaging by mobile C-arm with flat-panel detector‖. Journal of Spinal Disorders and Techniques. DOI: 10.1097/BSD.0b013e3182a357

Praveen Satarasinghe, Kojo D. Hamilton, Michael J. Tarver, Robert J. Buchanan and Michael T. Koltz. 2012. Thoracic, Lumbar and Sacral Pedicle Screw Placement Using Stryker-Ziehm Virtual Screw Technology and Navigated Stryker Cordless Driver 3: Technical Note‖, J. Clin. Med. Vol. 84.

Gelalis I. D., Paschos N. K., Pakos E. E., Politis A. N., Arnaoutoglou C. M., Karageorgos A. C. 2012. Accuracy of pedicle screw placement: A systematic review of prospective in vivo studies comparing free hand, fluoroscopy guidance and navigation techniques. Eur. Spine J. 21, 247-255.

Gonzalvo A., Fitt G., Liew S. 2009. The learning curve of pedicle screw placement: How many screws are enough? Spine. 34, 761-765.

Zhao X., Zhao J., Xie Y., Mi J. 2016. The utility of a digital virtual template for junior surgeons in pedicle screw placement in the lumbar spine. BioMed Res. Int. 3076025.

Lee M. H., Lin M. H., Weng H. H.; Cheng W. C., Tsai Y. H., Wang T. C., Yang J. T. 2013. Feasibility of intra-operative computed tomography navigation system for pedicle screw insertion of the thoraco- lumbar spine. J. Spinal Disord. Tech. 26, E183-E187.

Kim Y. J., Lenke L. G., Bridwell K. H., Cho Y. S., Riew K. D. 2004. Free hand pedicle screw placement in the thoracicspine: Is it safe? Spine. 29, 333-342.

Hammer N., Glätzner J., Feja C., Kühne C. Meixensberger J., Planitzer U., et al. 2015. Human Vagus Nerve Branching in the Cervical Region. PLoS ONE 10(2): e0118006. doi: 10.1371/journal. pone.0118006

Heiner Martin, Ulf Bahlke, Albrecht Dietze, Volker Zschorlich, Klaus-Peter Schmitz and Thomas Mittlmeier. 2012. Investigation of first ray mobility during gait by kinematic fluoroscopic imaging-a novel method, Martin et al. BMC Musculoskeletal Disorders. 13: 14.

Nester C. J., Liu A. M., Ward E., Howard D., Cocheba J., Derrick T., Patterson P. 2007. Invitro study of foot kinematics using a dynamic walking cadaver model. J Biomech. 40: 1927-1937.

Nester C. J., Jones R. K., Liu A., Howard D., Lundberg A., Arndt A., Lundgren P., Stacoff A., Wolf P. 2007. Foot kinematics during walking measured using bone surface markers. J Biomech. 40: 3412-3423.

Lundgren P., Nester C., Liu A., Arndt A., Jones R., Stacoff A., Wolf P., Lundberg A. 2008. Invasive in vivo measurement of rear-, mid-, and forefoot motion during walking. Gait Posture. 28: 93-100.

2010. Robert Green Watkins, Akash Gupta, Cost-Effectiveness of Image-Guided Spine Surgery, Open Orthop J. 4: 228-233.

Esses S. I., Sachs B. L., Dreyzin V. 1993. Complications associated with the technique of pedicle screw fixation. Spine. 18: 2231-9.

Wang J. C,, Mummaneni P. V., Haid R. W. 2005. Current treatment strategies for the painful lumbar motion segment: posterolateral fusion versus interbody fusion. Spine. 30: S33-S43. [PubMed] [Google Scholar]

Castro W., Halm H., Jerosch J., Malms J., Steinbeck J., Blasius S. 1996. Accuracy of pedicle screw placement in lumbar vertebrae. Spine. 21: 1320-4.

Farber G. L., Place H. M., Mazur R. A., Jones DEC, Damiano T. R. 1995. Accuracy of pedicle screw placement in lumbar fusions by plain radiographs and computer tomography. Spine. 20: 1494-9.

Gertzbein S. D., Robbins S. E. 1990. Accuracy of pedicle screw placement in vivo. Spine. 15: 11-14.

Guven O., Yalcin S., Karahan M., Sevinc T. T. 1994. Postoperative evaluation of transpedicular screws with computed tomography. Orthopedic Rev. 511-6.